

Tensile Behaviour of Slag-based Engineered Cementitious Composite

Chai Lian Oh^{1*}, Siong Wee Lee², Norrul Azmi Yahya¹, Gajalakshmi Pandulu³ and Mohd Raizamzamani Md Zain¹

¹*School of Civil Engineering, College of Engineering, Universiti Teknologi MARA, 40450 UiTM, Shah Alam, Selangor Darul Ehsan, Malaysia*

²*School of Civil Engineering, College of Engineering, Universiti Teknologi MARA Johor, Pasir Gudang Campus, 81750 UiTM, Masai, Johor, Malaysia*

³*School of Infrastructure, B.S. Abdur Rahman Crescent, Institute of Science & Technology (BSACIST) Vandalur, Chennai-600 048, Tamil Nadu, India*

ABSTRACT

Engineered Cementitious Composites (ECC) have become another alternative in the concrete industry due to their excellent strain capacity under uniaxial tension. Research and development for new ECC mix incorporating wastes remain open to fulfil the industrial needs to produce green and sustainable ECCs. This paper presents the experimental work on the tensile and cracking behaviour of ECCs utilising industrial waste, namely ground granulated blast-furnace slag (GGBS), to replace cement. A total of four slag-based ECC mixes containing 2%–2.5% of PVA fibres and 50%–60% GGBS were investigated under uniaxial compressive and tensile tests. Compressive strength, tensile strength and the

crack behaviours of the slag-based ECCs were evaluated and compared with a control mix. The experimental results show that the slag-based ECCs can achieve tensile strain capacity 2.6%–2.75% and ultimate tensile strength 1.43 MPa–2.82 MPa at 28 days. It was also found that the ECCs with GGBS and fibres formed few hairline cracks at the gage of the dog bone compared to brittle fracture in the control specimens.

Keywords: Crack, engineered cementitious composites, fibre, slag, tensile

ARTICLE INFO

Article history:

Received: 2 August 2021

Accepted: 12 November 2021

Published: 15 December 2021

DOI: <https://doi.org/10.47836/pjst.30.1.17>

E-mail addresses:

chailian@uitm.edu.my (Chai Lian Oh)

leesiongwee@uitm.edu.my (Siong Wee Lee)

norrulazmi@uitm.edu.my (Norrul Azmi Yahya)

gajalakshmi@crescent.education (Gajalakshmi Pandulu)

raizam@uitm.edu.my (Mohd Raizamzamani Md Zain)

*Corresponding author

INTRODUCTION

All over the world, the Ordinary Portland Cement (OPC) is used widely as a construction material, especially in concrete buildings and infrastructure. However, the manufacturing process of OPC can release carbon dioxide into the atmosphere, subsequently negatively impacting the environment. In order to lessen the pollution issues and excess embodied energy utilisation, supplementary cementitious material can be utilised for the construction works. The industrial alumina-silicate by-product materials are employed for landfilling purposes, such as fly ash, ground granulated blast furnace slag (GGBS) etc. (Sakulich, 2011). Research works have also been carried out by utilising these aluminosilicate by-product materials in concrete as a partially replacing material to ease the idea of combining the eco-friendly materials, leading to a sustainable built environment.

Engineered Cementitious Composites (ECC), popularly known as bendable concrete, was introduced in the 1990s with the motivation to improve the tensile properties of concrete. The design of the ECC mix requires careful constituent tailoring and optimisation. Important constituents in ECC are cement, Polyvinyl Alcohol (PVA) fibres, silica sand, water and superplasticiser. Superior ductility of the innovation has made it attractive for both seismic and non-seismic applications (Li, 2003).

Many have investigated the tensile properties and cracking behaviour of ECCs. For instance, Kim et al. (2007) investigated strain-hardening behaviour in uniaxial tension of ECC containing GGBS at moderate strength. The tensile strain capacity of slag-based ECC was 50% higher than that of the conventional ECC. It was due to the support of the slag particles in the improvement of dispersion of fibres. Ma et al. (2015) studied the tensile properties of ECCs using local materials, including 2% volume PVA fibre, fly ash and crumb rubber. The authors successfully developed ECCs with up to 5 MPa ultimate tensile strength and up to 6% tensile strain capacity. Also, it was observed that a cost-effective ductile ECC could be designed by using local materials as ingredients. Finally, Chen et al. (2013) tested four ECCs incorporating GGBS at a range of 50% to 80% for the tensile, quasi-static and dynamic compressive performances. The findings from the research showed that the increase of GGBS content in ECCs increased the tensile strain capacity but reduced the ultimate tensile strength and average crack width. Booya et al. (2020) evaluated the mechanical performance of ECC using slag and fly ash as cement replacement materials. The experimental test results showed that both the slag- and fly ash-based ECC displayed similar strain-hardening and ductility characteristics but demonstrated different performance in drying shrinkage strains. Zhu et al. (2012) developed green ECC combination mineral admixtures of fly ash and GGBS with high tensile ductility and good matrix strength at an early age. Nguyễn et al. (2020) evaluated the healing performance of three ECC mixtures utilising a different proportion of Portland cement, CaO-based expansive agent and GGBS. It was found that all the ECCs showed comparative high compressive strength

(> 90MPa), tensile strength (> 8 MPa), and tensile strain (> 4.5%). Kumar and Ranade (2021) developed ECC with slag and calcium carbonate powder. Tensile performance of mixtures with different slag-to-cement weight ratios (1.5 to 3.5) and combination with 25 μm calcium carbonate powder was studied, and it was found that the mixtures with a ratio of slag-to-cement 2.0 to 2.5 demonstrated higher tensile strain capacity and modulus rupture. The authors studied the mechanical properties of ECCs using local constituents from Malaysia (Lee, Oh, & Md Zain, 2019; Lee et al., 2018; Lee, Oh, Zain, et al., 2019). The results showed that the ECC with GGBS of 60% replacing cement achieved higher tensile strength and tensile strain capacity than other percentages (50% and 70%). A review of tensile properties of ECCs could be found in Yu et al. (2018).

Enhancement in tensile strength of ECC after incorporation of slag can be seen through the studies above. However, there are no conclusive results of the slag volume on ECC's tensile strength and cracking behaviour. Thus, this paper investigates experimentally the tensile properties of a series of ECCs containing 50% and 60% local GGBS replacing the cement. The ECCs were also designed to have PVA volume fractions of 2.0 % and 2.5 %. A total of four ECC mixes containing different percentages of PVA fibres and GGBS, as well as a control mix, were prepared and tested under uniaxial compression and tensile tests. This study investigated the effects of slag volume on the tensile properties of ECCs, which were specifically designed for concrete applications.

METHODOLOGY

This section presents the methodology of the experimental works in four main phases: (1) mix design of ECC, (2) preparation of materials, (3) preparation of specimens and (4) testing.

Mix Design of ECC

A total of four (4) slag-based ECC mixtures incorporated GGBS were designed. GGBS was chosen as the slag material to replace the cement volumes in the ECCs partially. Several important parameters were considered in the mix design to ensure the strength and durability of the ECCs. In this study, four ECC mixtures were mainly differentiated with the cement ratios to GGBS and the fibre volume fraction. The ECC mixtures were designed with ratios of cement to GGBS of 1.0 and 0.67 as well as the volume fraction of fibre of 2.0% and 2.5%. In addition, the sand-to-cement ratio and water-cement ratio was set to 0.2 and 0.27, respectively. Table 1 shows the mix composition for four (4) ECC mixes (i.e. G50F2.0, G50F2.5, G60F2.0 and G60F2.5) and one control mix (i.e. Control). The name of the mix reflects the mix composition. For instance, G50F2.0 indicates that the mix contains GGBS of 50% replacing cement and PVA fibre 2.0% volume fraction. There was neither GGBS nor PVA fibre applied in the control mix. The design mix resulted in a density of ECCs ranging from 2133 to 2160 kg/m^3 .

Table 1

Mix composition (kg/m³)

Mix	Cement	GGBS	Silica sand	Water	PVA Fibre	Superplasticizer	Density
G50F2.0	722	722	289	390	26	10	2160
G50F2.5	719	719	288	388	32	10	2156
G60F2.0	575	863	288	388	26	10	2149
G60F2.5	572	858	286	386	32	10	2145
Control	1444	0	289	390	0	10	2133

Materials

Cement, GGBS, silica sand, PVA fibre, water and superplasticiser are the key materials used in producing ECCs in this study. The specifications of these materials are detailed as follows:

Cement—Ordinary Portland Cement (OPC) type CEM I 42.5N confirming to MS EN 197-1 standard, which is good for general purposes, was used.

GGBS—Ground Granulated Blast Furnace Slag (GGBS), an industrial by-product from the blast-furnaces, is widely known for low embodied CO₂ and acts as a hydraulic binder like cement. GGBS was used to partially replace the cement at 50% and 60% in the study as a sustainable alternative to cement. The chemical compositions and density of both OPC and GGBS are shown in Table 2.

Silica sand—From local silica sand deposits, the silica sand was used as fine aggregate in ECC mixtures. The average particle size of silica sand used is 285 microns.

Fibres—PVA fibre, namely Kuralon™ RECS15 from Kuraray, Japan, was used. The fibre is specified with 40-micron diameter, 12 mm length, 1.6 GPa tensile strength and 40 GPa Modulus. In addition, the Resin-Bundled type fibre with better dispersibility was chosen to prevent any re-aggregation and balling of fibres during the mixing process.

Table 2

Density and chemical composition

Chemical compositions	Unit	OPC	GGBS
Silica (SiO ₂)		12.80	35.67
Alumina (Al ₂ O ₃)	%	2.13	10.15
Calcium Oxide (CaO)		77.53	43.68
Magnesia (MgO)		0.96	4.03

Table 2 (Continue)

Chemical compositions	Unit	OPC	GGBS
Potassium Oxide (K ₂ O)		0.53	0.29
Iron oxide (Fe ₂ O ₃)	%	1.61	3.12
Sulphur trioxide (SO ₃)		3.80	2.69

Superplasticizer–Superplasticizer is commonly known as a high range water reducer. The superplasticiser MasterGlenium SKY 8705 was added to the mixture. The superplasticizer contains polycarboxylate ether polymers, Chloride ion content < 0.2%, pH > 6, reddish-brown liquid and complies with BS EN934: Part 3: 1985. It is beneficial to concrete, such as allowing slump retention and enhancing the mechanical properties of concrete produced in hot climates.

Preparation of Specimens

Cylinder and dog bone specimens were assessed at concrete age of 28 days under uniaxial compressive and uniaxial tensile tests, respectively. Cylinder and dog bone specimens are widely used in uniaxial compression and tensile tests for ECC (Booya et al., 2020; JSCE, 2008; Meng et al., 2017; Yu et al., 2018). JSCE (2008) recommended that the cylinder specimens of 50 mm in diameter and 100 mm in height be used in the uniaxial compression test if the mix does not consist of coarse aggregates. Thus, the cylinder specimens with the recommended size were used since only silica sand was used in the study. For tensile specimens, the dog bone specimens with width, height, the thickness of 40 mm, 320 mm and 13 mm were prepared considering the recommendations in JSCE (2008). Moulds for cylinder specimens were made by PVC type with an inner diameter of 50 mm, whereas dog bone specimens were fabricated in metal form. The specimen moulds and dimensions of dog bone are shown in Figure 1.

After the fabrication of specimen moulds, the casting of ECCs was carried out through a few main steps. First, solid ingredients, such as cement, GGBS and silica sand, were mixed for two minutes using a mixing machine. The water and superplasticiser were then added gradually to obtain a consistent and uniform mixed ECC. This process took about three minutes. Later, the PVA fibre was added slowly to allow good distribution of fibre during the mixing. It was followed by the fresh ECC into the moulds. The mould with fresh ECC was then compacted using the vibration table to expel entrapped air from freshly placed for about one minute. Detachment of the specimens from their moulds took place 24 hours after placement. Finally, the specimens were covered, placed, and cured in dry and normal room condition.

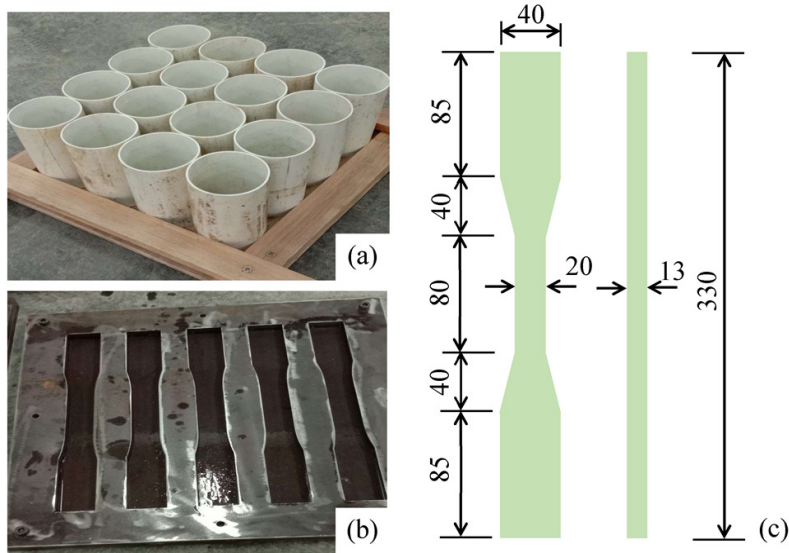


Figure 1. Specimen preparation: (a) cylinder moulds, (b) dog bone moulds and (c) dog bone dimensions (mm)

Testing

This section presents two main testing in the experimental work: uniaxial compression test and uniaxial tensile test, which are in accordance with (JSCE, 2008). Observing the crack widths using a microscope was also carried out during and after the uniaxial tensile test. JSCE (2008) recommended that at least three specimens be prepared for the uniaxial compression test and at least five for the uniaxial tensile test. The numbers of the test specimen for uniaxial compression and tensile tests in this study are as shown in Table 3.

Table 3
Numbers of test specimens

Test	G50F2.0	G50F2.5	G60F2.0	G60F2.5	Control
Uniaxial Compression Test	5 nos.				
Uniaxial Tensile Test	5 nos.				

Uniaxial Compression Test. The compression test was conducted for five cylindrical specimens of each mix at 28 days using a UTM-1000 Universal Testing Machine (Figure 2a). First, the surfaces of a cylinder specimen and the bearing surface of the testing machine were cleaned. The cylinder specimen was then placed at the centre of the base plate. Next, the load was applied with a loading rate of 0.5 mm/min. The load was applied incrementally and continuously to the specimen, and the data was stored in a computer.

Uniaxial Tensile Test. A tensile test was performed on five dog bone specimens for each mix at 28 days of curing using Shimadzu AGX Universal Testing Machine with a capacity of 50kN. The test set up for the uniaxial tensile test was arranged in accordance with JSCE (2008), which is shown in Figure 2b. The dog bone specimen was placed in the machine with a fixed support at one end and a pin (hinge support) on the other end. The specimen was adjusted and aligned properly vertically between the chucks at the machine so that the tensile load was applied at the centroidal axis of the specimen. The tests were performed at a cross-head displacement rate of 0.3 mm/min. During the tests, the machine continuously recorded the tensile loads (N) and corresponding elongation (mm). Tensile stress was obtained by dividing the load by the initial sectional area, which the area was calculated based on the mean value of three sections at both ends and centre of the specimen. The strain was determined by dividing the elongation of the specimen by the gauge length.



Figure 2. Testing set-up (a) uniaxial compression test and (b) uniaxial tensile test

The crack occurrence was observed during the uniaxial tensile test. Crack widths of the dog bone specimen were measured instantly after the uniaxial tensile test using a Crack Detection Microscope with an optical magnification of X40 and a sensitivity of 0.02mm. Only the maximum and minimum crack widths were recorded. The crack patterns on the dog bone specimens were also observed. The quantities of cracks before and after the test were recorded. It is to ensure the crack observation is properly detailed; either the cracks happen during the hardening process or in the old specimens.

RESULTS AND DISCUSSION

This section discusses the results obtained from the uniaxial compression and tensile test in the experimental works. The results in terms of compression strength, tensile stress-strain relations and cracking behaviour are presented.

Compressive Strength

The compressive strength of ECCs and control specimen obtained at concrete age of 28 days is presented in Figure 3. The percentage of differences for the compressive strength of the ECCs compared to the control are shown in Table 4.

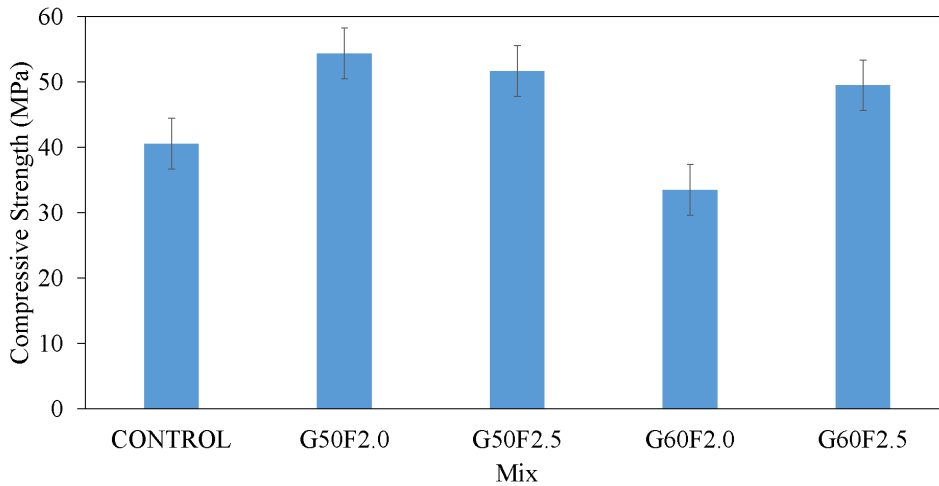


Figure 3. Compressive strength of ECCs

Table 4

Percentage of difference of ECCs in compressive strength

Mix	Average Compressive Strength (MPa)	Percentage of difference (%)
Control	44.02 (1.33)	-
G50F2.0	57.02 (2.63)	29.5
G50F2.5	54.82 (2.22)	24.5
G60F2.0	35.92 (3.15)	-18.4
G60F2.5	52.69 (2.57)	19.7

It was found that G50F2.0 achieves the highest compression strength of 57.02 MPa (29.5% higher than the control), whereas G60F2.0 achieves the lowest compression strength of 35.92 MPa (18.4% lower than the control). Furthermore, all the ECCs except G60F2.0 have higher compressive strength compared to the control of 19.7–29.5%. It indicates that incorporating fibre at either 2.0% or 2.5% volume fraction in ECCs has generally enhanced the compressive strength of the concrete. Additionally, at same fibre volume fraction, ECCs with 60% percentage GGBS (i.e., G60F2.0 and G60F2.5) achieve lower

compression strength compared to ECCs with 50% GGBS (i.e., G50F2.0 and G50F2.5) in the study. The trend where compression strength of the ECCs decreases as GGBS content in ECC increases is consistent with Kumar and Ranade (2021). The reduction of compressive strength when having beyond 60–80% of GGBS as cement replacement level may be due to inaccessibility free calcium hydroxide for pozzolanic reaction or formation of low-density C-S-H gel by GGBS particles (Kumar & Ranade, 2021).

Cracks Patterns

The cracking behaviour of the ECC specimen was evaluated based on the uniaxial tensile test. Figure 4 shows the crack patterns for the specimens after failure. Only the control, G50F2.0 and G60F2.0 specimens were presented owing to a similar crack pattern in all the ECC specimens. Occurrence of the first crack at the gage of the dog bone at the first crack strength was observed in ECC specimens. It follows by observing a few hairline cracks formed near the first crack (at the gage of dog bone) in ECC specimens. The formation of hairline cracks was associated with inelastic strain during the test. After the ECC specimens reached the ultimate tensile strength, the composite experienced a localised crack, which caused the composite to fail. Meanwhile, under incremental tensile loading, the control specimens failed in a fracture before any form of cracks. Four out of five control dog bone specimens were broken at the gage, either at the middle or near the shoulder. The tensile stress-strain relation and crack observation reveal that the control specimens are brittle and have low tensile strain compared to the ECCs.

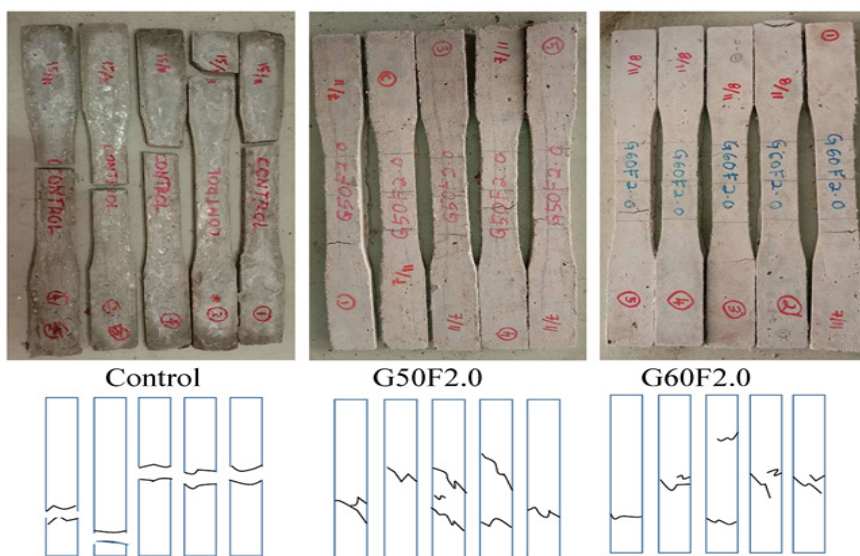


Figure 4. Cracking behaviour of specimens in series Control, G50F2.0 and G60F2.0

Table 5 shows the maximum crack width of the ECCs specimens after failure. Maximum crack widths ranging from 0.5 mm to 1.2 mm were recorded in ECC specimens. The control specimens were broken into two parts (or fracture) during the uniaxial tensile test before any form of cracks; thus, no crack width results were available. The average maximum crack width increased with the increase of the GGBS content from 50% to 60%. Decrement of maximum crack width was observed when the volume fraction of fibre increased from 2.0% to 2.5%. However, the fibre (2.0–2.5%) to the crack control of the ECCs is not as dominant as compared to the effect of GGBS (50–60%) in this study. Therefore, the maximum crack width of the ECCs is higher than the recommendations from JSCE (2008) of 0.1mm for fibre reinforced concrete and EN2 (2004) of 0.3mm for normal reinforced concrete.

Table 5

Maximum crack width of dog bone specimens

Mix	Maximum crack width (mm)					Average
	S1	S2	S3	S4	S5	
Control	F	F	F	F	F	NA
G50F2.0	0.6	0.7	-	-	0.6	0.63
G50F2.5	-	0.5	0.5	0.5	0.5	0.50
G60F2.0	1.0	-	1.2	-	1.0	1.07
G60F2.5	-	1.0	-	1.0	1.1	1.03

Tensile Stress-strain Relation

The typical tensile stress-strain curves of the ECCs and control specimens obtained from the uniaxial tensile test are shown in Figure 5. The first crack strength, ultimate tensile strength and tensile strain capacity were labelled. There are three primary regions in the tensile stress-strain curves of ECCs, regions AB, BC and CD. In region AB, the curve starts to progress in a linearly increasing trend indicating an occurrence of elastic deformation in the specimen at this stage, till the first cracking. The steeper of slope in this region reveals the stiffer the material. Next, the curve in region BC advances in a gradual increasing and nonlinear manner showing pseudo strain hardening behaviour of the material. Fluctuation in the curve in region BC is mainly due to the development of multiple micro-cracks, the propagation of cracks observed associated with the fibre extraction in the specimen at an increasing inelastic strain. When one of the cracks becomes critical, localisation of the crack results in the decrement of tensile stress after C. Region CD presents a descending curve, which is also the effect of the enlargement of the critical crack with continuous application of load. Point D is recorded as the failure of the ECCs. It is clearly seen from

the tensile stress-strain relations that all ECC specimens show pseudo strain hardening behaviour compared to the control specimen. It is expected that the inclusion of the fibre at an optimum volume fraction of and interaction between the fibre-matrix can induce multiple cracking in ECC (Kumar & Ranade, 2021; Meng et al., 2017; Yu et al., 2020). The stress-strain curve for the control specimen illustrates slight fluctuation right after the first cracking; however, it hardly demonstrates the strain hardening behaviour. The curve rises steeply to the peak at a small strain without much fluctuation, indicating no development of other cracks in the specimen. It is supported by the observation of the specimen during the test, where only a critical crack was detected, mostly located at the gauge of the control specimen. Observation of the brittle fracture that suddenly occurred that led to the failure of the control specimen could explain why there is a steep fall in the curve after achieving ultimate tensile strength.

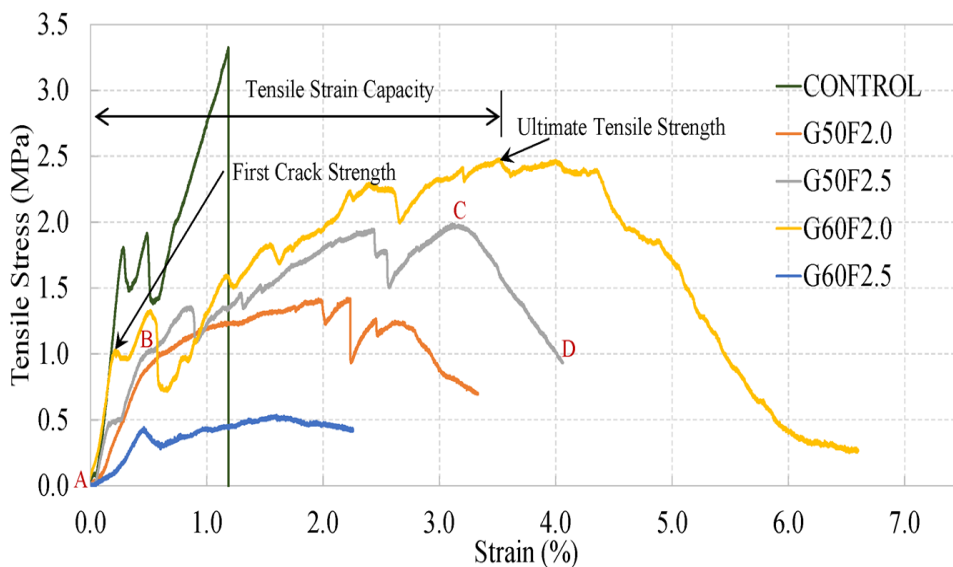


Figure 5. Tensile stress-strain curves

Table 6 shows the uniaxial tensile test of first crack strength, ultimate tensile strength, and ultimate tensile strain capacity. It was found that the control specimen exhibits higher first crack strength and ultimate tensile strength at 28 days compared to the ECC specimen. As expected, the control specimens attained the lowest tensile strain capacity, which explains the observations regarding the brittle fracture in the specimens.

Overall, ECC specimens G50F2.0, G50F2.5 and G60F2.0 demonstrated tensile strain capacity ranging from 2.6 %–2.75 % and with an ultimate tensile strength at a range of

1.43 MPa–2.82 MPa. Effect of fibres can be clearly seen when there was an occurrence of microcracking in ECCs compared to a dominant localised brittle fracture in the control specimen (without fibres). Additionally, ECCs achieve enhanced tensile strain capacity up to 1.6 times higher than the control specimens and about 200–300 times higher than the conventional concrete, which is around 0.01% (Nguyễn et al., 2020). For ECCs with 50% GGBS, when fibre volume fraction increased from 2.0% to 2.5%, increment of 20.6% in first crack strength and 32.9% in ultimate tensile strength was observed, however, with a 7.3% decrement in the tensile strain capacity. The enhanced strength can be supported with the fibre bridging effect, in which the crack propagation is controlled by fibres (Du et al., 2020).

The influence of GGBS can be observed in ECCs with a fibre volume fraction of 2.0%. When GGBS content increased from 50% to 60%, enhancement in tensile properties of ECC were observed, such as 6.5% increment in first crack strength, 97.2% increment in ultimate tensile strength and 5.76% increment in tensile strain capacity. The results are in good agreement with previous experimental works (Chen et al., 2013; Kim et al., 2007; Kumar & Ranade, 2021). According to Chen et al. (2013); Kumar and Ranade (2021), the addition of slag can reduce the toughness of the matrix, which contribute to higher multiple cracking. Furthermore, incorporating slag enhances the fibre-matrix interaction (Kumar & Ranade, 2021) and fibre dispersion (Kim et al., 2007), resulting in higher tensile strain capacity.

In this study, G60F2.5 exhibits relatively low tensile properties compared to other ECC specimens. The variation of the tensile properties is most likely due to variation in fibre bridging properties, matrix flaw randomness and excessive un-hydrated slag particles. Matrix flaws can be affected by the mixing process, vibration time and other factors (Meng et al., 2017). In addition, un-hydrated slag particles due to excessive slag particles can weaken the bonding of fibre-matrix (Kumar & Ranade, 2021).

Table 6

Tensile properties of ECCs

Mix	First Crack Strength (MPa)	Ultimate Tensile Strength (MPa)	Tensile strain capacity (%)
Control	1.95 (0.65)	3.27 (0.23)	1.15 (0.15)
G50F2.0	0.92 (0.07)	1.43 (0.07)	2.60 (0.69)
G50F2.5	1.11 (0.91)	1.90 (0.13)	2.41 (0.98)
G60F2.0	0.98 (0.18)	2.82 (0.38)	2.75 (0.93)
G60F2.5	0.50 (0.11)	0.61 (0.08)	1.40 (0.28)

Note: Values between parentheses is the standard deviation of the mean.

CONCLUSION

This study presents experimental work for the tensile properties and cracking behaviour of ECCs containing different volumes of GGBS and fibre. Few conclusions can be made from the study:

- a. Most slag-based ECCs have higher compressive strength than the control of increment up to 29.5%. ECCs with 50% GGBS have higher compression strength compared to ECCs with 60% GGBS in the study.
- b. All ECC specimens demonstrate pseudo strain hardening behaviour. Most of the ECCs demonstrated tensile strain capacity ranging from 2.6%–2.75% and ultimate tensile strength with a range of 1.43 MPa–2.82 MPa. These ECCs demonstrate tensile strain capacity up to 1.6 times higher than control in this study.
- c. The control specimen demonstrated brittle fractured before any form of cracks, whereas ECCs with GGBS and fibres formed few hairline cracks at the gage of the dog bone. Higher GGBS in the specimen resulted in higher maximum crack width.

Few recommendations were made from the study where research on the effect of different sizes of fibres, silica sand, more variety percentage of replacement materials, different waste materials etc. is needed to gain a deeper understanding of their relationship with tensile and cracking behaviours and to develop more quality and sustainable ECCs for structural applications.

ACKNOWLEDGMENTS

The Universiti Teknologi MARA funded this research under grant Research Entity Initiative (REI) 600-IRMI/REI 5/3 (012/2018). The authors gratefully acknowledge undergraduate student *Najihah binti Sukri* for assisting in the laboratory works. In addition, the authors would also like to thank the School of Civil Engineering, College of Engineering, Universiti Teknologi MARA, Shah Alam, Selangor.

REFERENCES

- Booya, E., Gorospe, K., Das, S., & Loh, P. (2020). The influence of utilizing slag in lieu of fly ash on the performance of engineered cementitious composites. *Construction and Building Materials*, 256, Article 119412. <https://doi.org/https://doi.org/10.1016/j.conbuildmat.2020.119412>
- Chen, Z., Yang, Y., & Yao, Y. (2013). Quasi-static and dynamic compressive mechanical properties of engineered cementitious composite incorporating ground granulated blast furnace slag. *Materials & Design*, 44, 500-508. <https://doi.org/https://doi.org/10.1016/j.matdes.2012.08.037>
- Du, Q., Cai, C., Lv, J., Wu, J., Pan, T., & Zhou, J. (2020). Experimental investigation on the mechanical properties and microstructure of basalt fiber reinforced engineered cementitious composite. *Materials*, 13(17), Article 3796. <https://doi.org/10.3390/ma13173796>

- Kim, J. K., Kim, J. S., Ha, G. J., & Kim, Y. Y. (2007). Tensile and fiber dispersion performance of ECC (engineered cementitious composites) produced with ground granulated blast furnace slag. *Cement and Concrete Research*, 37(7), 1096-1105. <https://doi.org/https://doi.org/10.1016/j.cemconres.2007.04.006>
- Kumar, D., & Ranade, R. (2021). Development of strain-hardening cementitious composites utilizing slag and calcium carbonate powder. *Construction and Building Materials*, 273, Article 122028. <https://doi.org/https://doi.org/10.1016/j.conbuildmat.2020.122028>
- Lee, S. W., Oh, C. L., & Zain, M. R. M. (2019). Mechanical properties of engineered cementitious composites using local ingredients. *Journal of Mechanical Engineering (JMEchE)*, 16(2), 145-157. <https://doi.org/10.21491/jmeche.v16i2.15332>
- Lee, S. W., Oh, C. L., & Zain, M. R. M. (2018). Evaluation of the design mix proportion on mechanical properties of engineered cementitious composites. In *Key Engineering Materials* (Vol. 775, pp. 589-595). Trans Tech Publications Ltd.
- Lee, S. W., Oh, C. L., Zain, M. R. M., Yahya, N. A., & Rahman, A. A. (2019). Mechanical performances of green engineered cementitious composites incorporating various types of sand. In *Key Engineering Materials* (Vol. 821, pp. 512-517). Trans Tech Publications Ltd.
- Li, V. C. (2003). On engineered cementitious composites (ECC) a review of the material and its applications. *Journal of Advanced Concrete Technology*, 1(3), 215-230. <https://doi.org/https://doi.org/10.3151/jact.1.215>
- Ma, H., Qian, S., Zhang, Z., Lin, Z., & Li, V. C. (2015). Tailoring engineered cementitious composites with local ingredients. *Construction and Building Materials*, 101, 584-595. <https://doi.org/https://doi.org/10.1016/j.conbuildmat.2015.10.146>
- Meng, D., Huang, T., Zhang, Y., & Lee, C. (2017). Mechanical behaviour of a polyvinyl alcohol fibre reinforced engineered cementitious composite (PVA-ECC) using local ingredients. *Construction and Building Materials*, 141, 259-270. <https://doi.org/10.1016/j.conbuildmat.2017.02.158>
- National Standard Authority of Ireland. (2005). *Eurocode 2: Design of concrete structures-part 1-1: General rules and rules for buildings*. British Standard Institution.
- Nguyễn, H. H., Choi, J. I., Park, S. E., Cha, S. L., Huh, J., & Lee, B. Y. (2020). Autogenous healing of high strength engineered cementitious composites (ECC) using calcium-containing binders. *Construction and Building Materials*, 265, Article 120857. <https://doi.org/https://doi.org/10.1016/j.conbuildmat.2020.120857>
- Sakulich, A. R. (2011). Reinforced geopolymer composites for enhanced material greenness and durability. *Sustainable Cities and Society*, 1(4), 195-210. <https://doi.org/https://doi.org/10.1016/j.scs.2011.07.009>
- Yokota, H., Rokugo, K., & Sakata, N. (2008). JSCE recommendations for design and construction of high performance fiber reinforced cement composite with multiple fine cracks. In *High Performance Fiber Reinforced Cement Composites*. Springer.
- Yu, K. Q., Lu, Z. D., Dai, J. G., & Shah, S. P. (2020). Direct tensile properties and stress - strain model of UHP-ECC. *Journal of Materials in Civil Engineering*, 32(1), Article 04019334. [https://doi.org/10.1061/\(ASCE\)MT.1943-5533.0002975](https://doi.org/10.1061/(ASCE)MT.1943-5533.0002975)

- Yu, K., Li, L., Yu, J., Wang, Y., Ye, J., & Xu, Q. (2018). Direct tensile properties of engineered cementitious composites: a review. *Construction and Building Materials*, 165, 346-362. <https://doi.org/https://doi.org/10.1016/j.conbuildmat.2017.12.124>
- Zhu, Y., Yang, Y., & Yao, Y. (2012). Use of slag to improve mechanical properties of engineered cementitious composites (ECCs) with high volumes of fly ash. *Construction and Building Materials*, 36, 1076-1081. <https://doi.org/https://doi.org/10.1016/j.conbuildmat.2012.04.031>

